

Very Bright, Enantiopure Europium(III) Complexes Allow Time-Gated Chiral Contrast Imaging

Received 00th January 20xx,
Accepted 00th January 20xx

Andrew T. Frawley,^a Robert Pal*^a and David Parker*^a

DOI: 10.1039/x0xx00000x

www.rsc.org/

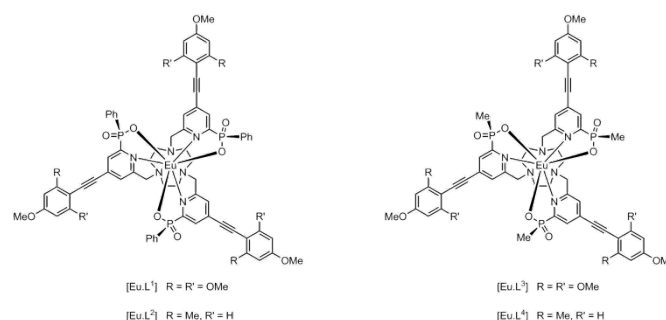
Chiral image contrast is demonstrated using enantiopure Eu(III) complexes that emit right or left-handed circularly polarised light of opposite sign, at selected wavelengths.

Photographic image contrast based on the relative intensity of emitted circularly polarised light is an unexplored phenomenon. Its observation requires a means of distinguishing left and right-handed circularly polarised light for which a pragmatic solution, in the absence of suitable broad spectrum chiral filters, is to use a quarter wave plate, linear polariser and an appropriate band-pass filter in the path of the observed light beam. Here, we describe the resolution of very bright, Eu(III) complexes by chiral HPLC, report the stability of the enantiopure complexes to racemisation and introduce a proof-of-concept study, revealing the ability to differentiate and detect objects labelled with an emissive Δ or Λ europium(III) complex using a time-gated camera, following near-UV flash excitation.

Circularly polarised luminescence (CPL) is the emission analogue of circular dichroism (CD) and intrinsically is a much more sensitive optical technique.¹⁻³ Emission dissymmetry factors, g_{em} , (given as $g = 2(I_L - I_R) / (I_L + I_R)$) are typically very small for helical organic molecules but can be as high as 1.4 for lanthanide(III) complexes.⁴ Such behaviour contrasts with the size of g_{abs} values measured in CD that rarely exceed 10^{-4} . The ease of observation of circularly polarised photoluminescence from a chiral lanthanide (III) complex is a function of the brightness, B , of that complex at a given excitation wavelength, ($B_{\lambda} \sim \epsilon_{\lambda} \phi_{em}$), and the nature of the lanthanide ion that determines the emission spectral form. Of particular importance, in this context, are the numerous series of water-soluble and highly emissive Eu(III) and Tb(III) complexes emitting in the visible region that are less prone to vibrational deactivation of the excited state and can be photosensitised from 337 to 405 nm.⁵⁻⁸

Recently, a family of very bright europium(III) complexes has been introduced that are as bright as red fluorescent protein in aqueous media.⁹⁻¹³ The systems comprise a well-shielded nine-coordinate Eu(III) complex, cooperatively bound to the three ring nitrogen atoms of 1,4,7-triazacyclononane, three pyridyl nitrogens and three phosphinate oxygen groups. The aryl-alkynyl groups in the pyridine 4-position give rise to an internal charge transfer transition, that permits excitation in the range 340 to 375 nm, allowing efficient population of the europium 5D_0 excited state. Earlier crystallographic and solution NMR studies revealed that the complexes exist as a racemate, with an $RRR-\Lambda-\delta\delta\delta$ or $SSS-\Delta-\lambda\lambda\lambda$ configuration, specifying the chirality at phosphorus, around the helical axis (Δ is equivalent to P in this sense) or in the three ring NCCN chelates, respectively.^{9,12,14}

We have prepared the series of complexes, $[Eu.L^{1-4}]$, in which either a P -phenyl or P -methyl group is present; the former series is the more lipophilic. The nature of the peripheral phenyl substituents has also been varied, allowing the excitation wavelength to be shifted closer to 355 or 365 nm, which are more appropriate for laser or LED excitation.



The complexes were prepared using previously published methods,^{11,14} and were purified by reverse-phase HPLC. The brightness of each complex in methanol solution at 355 nm falls in the range 14.5 to $33 \text{ mM}^{-1} \text{ cm}^{-1}$ (Table 1 and Figure 1). The broad absorption bands mean that at 365 nm (LED) the absorbance of the complexes of $[Eu.L^1]$ and $[Eu.L^3]$ was $92(\pm 2)\%$ of that measured at 355 nm. Each of the complexes dissolves readily in methanol solution and could be resolved

^a Department of Chemistry, Durham University, South Road, Durham DH1 3LE, UK
E-mail: david.parker@durham.ac.uk, robert.pal@durham.ac.uk

*Electronic Supplementary Information (ESI) available: Complex synthesis, optical measurements, microscope technical details. See DOI: 10.1039/x0xx00000x

using chiral HPLC, with columns based on chloro-substituted phenylcarbamate derivatives of cellulose or amylose (ChiralPak IC or ID: *ESI*). The enantiomeric complexes eluted on the semi-preparative column with retention times differing by 8 to 18 minutes (295 K, MeOH, 4.4 mL/min).

FIG. 1 & TABLE 1.

The absolute configuration was assigned by comparison of their CPL spectra (Figure 2), assessing the sign and sequence of observed transitions in these spectra, with those measured for the parent systems, i.e. [Eu.L⁵] and [Eu.L⁶], that lack the alkynyl-aryl moiety. Configurational assignment of these archetypal complexes has been established by X-ray crystallography and CD studies in earlier work.^{9,14}

STRUCTURES OF [Eu.L⁵] and [Eu.L⁶]

The high signal intensity allowed the rapid measurement of the less commonly observed ⁵D₀-⁷F₅ CPL transitions (ca. 755 nm), as well as CPL associated with transitions from ⁵D₁ to ⁷F_{2,3,4}. No CPL signal was observed for the ⁵D₁-⁷F_{0,1} transitions, and the ⁵D₀ to ⁷F₆ manifold was not observed.

FIG 2

The stability of the resolved complexes to thermally-activated racemisation was examined in methanol, monitoring the appearance of the enantiomeric europium complex by analytical HPLC. No evidence for racemisation had been observed in solution at room temperature, but at 60 °C the half-life for racemisation could be measured and was found to be 410 h for [Eu.L⁴]. For [Eu.L²], less than 0.5 % of the other enantiomer could be discerned by chiral HPLC after 21 days under these conditions. These rates were independent of complex concentration, consistent with an intramolecular process, presumably involving stepwise dissociation of the Eu-oxygen bonds leading to epimerisation at each of the P centres, and a subsequent ring inversion of the triazacyclononane ring configuration ($\delta\delta\delta$ to $\lambda\lambda\lambda$). The half-life for racemisation of [Eu.L⁴] was considerably longer than that previously recorded for the parent complex (see *ESI*).^{14a}

Time-gated photography has been achieved using an off-the-shelf DSLR camera (Nikon D5300) equipped with an i-TTL flash unit (Nikon SB910) paired with a wireless flash trigger and receiver (YN-622N). The complex [Eu.L¹], fluorescein and a co-spot of both compounds were applied to non-optically brightened white paper as a solution in methanol and allowed to dry in air, creating a three-spot test paper (Scheme 1). A normal photograph under UV excitation shows, as expected, three spots of different colours (red from [Eu.L¹], green from fluorescein and yellow from the co-spot). Introduction of a band pass filter (595 ± 5 nm) to the camera, led to partial disappearance of the fluorescein spot, and all of the green-coloured emission, leaving three red spots. Total loss of the fluorescein spot was not achieved due to the long tail of the fluorescein emission. However, using distance-based time gating, placing the object 1.8 m from the camera (speed of light is 0.3 m/ns), the fluorescein spot was not observed, leaving just emission from [Eu.L¹].

SCHEME 1

Chiroptical contrast based imaging, i.e. the separation of left and right handed circularly polarised light emitted by the

separate Λ - and Δ -[Eu.L²] enantiomers has been facilitated via modification of a time-resolved Zeiss Axiovert 200M epifluorescence microscope set-up.¹⁵ Enantiopure Λ - and Δ -[Eu.L²] were deposited onto white paper containing no optical-brightener as solutions in methanol, and were allowed to dry at room temperature. Using our proof of concept time resolved DSLR camera (Scheme 1) areas of the two enantiopure [Eu.L²] spots with equal brightness for imaging were selected (see *ESI*). The microscope is equipped with a variable pulse sequence generator, which allows both CW and time-resolved operation. Acquisition using an EO-M(monochrome) 0.7M pixel rolling shutter camera was set at 7.2 ms per frame, and a typical value for time gating was 6-10 μ s, after pulsed excitation with a 365 nm UV LED (24 V, 1.2 W, *ESI*).

The microscope set up comprises an even number of polished-Al mirrors (Thor Labs), after circularly polarised light translation that are used to guide the emitted light to the detectors (imaging 2D-CCD, spectral 1D-CCD and lifetime assigned photomultiplier tube). It is important to note that the transmission/DIC imaging de Sénarmont compensator of the microscope has been eliminated. The absence of this component is a vital requirement, as such a rotatable optical element consists of two broad quarter-wave plates, and the linear polariser would severely limit chiroptical selection.

The microscope is equipped with a 395 nm dichroic mirror to allow epifluorescence detection. The integral emission filter (placed in front of the detector) has been swapped for a broad (400 – 800 nm) wavelength, 10 mm aperture quarter-wave plate, which allows incident angle based translation of circularly polarised light into linearly polarised light. Left-handed CPL is translated to vertical linearly polarised light (V-LPL), whilst right-handed CPL is translated to horizontal LPL. The unavoidable aperture restriction, due to the nature of the commercially available quarter-wave plate, has been compensated for with a pair of variable irises and a beam expander lens pair, in a linear arrangement between the 10x objective and the filter cube, to eliminate light loss in the detection arm. The final optical element to be introduced into the set-up is a pair of linear polarisers that allow selection and differentiation of vertically and horizontally polarised linear light. In this proof of concept instrument, we have employed a pair of pre-aligned 1" optical polarisers (40000:1 extinction ratio, Thor Labs.) in a 90° orientation. It is possible that one rotatable polariser could eliminate the need for the two individually aligned polarisers incorporated into a sliding filter-holder. However, a minimal rotational difference would contribute a significant error in contrast based chiroptical separation.

FIG. 3

Various microscopy images were taken (Fig. 3) illustrating both time gating and chiroptical selection. Images (A) and (B) show racemic [Eu.L¹] and fluorescein and demonstrate that time gating, as shown in Scheme 1 with the DSLR camera, is also possible using optical microscopy. Images (C) and (D) show the two enantiomers of [Eu.L²] with time gating and emission wavelength selection, whilst (E) and (F) introduce the

chiroptical selection. Image (E) shows that when selecting for right circularly polarised light, the top piece of paper with Λ -[Eu.L²] is brighter than the bottom. The CPL spectrum of [Eu.L²] (Fig. 2) shows strong negative CPL for the Λ -enantiomer at the wavelength of interest (~ 590 nm, $\Delta\epsilon = 1$ transition), corresponding to more right-handed CPL. The reverse behaviour is shown in image (F). For racemic [Eu.L¹], constant image brightness was observed irrespective of which channel was selected.

In conclusion, using a very bright Eu complex to provide CPL with a predominant handedness of circular polarisation between 585 and 605 nm, we have demonstrated the concept of chiral image contrast in emission. Chiral liquid crystal displays (LCDs), especially nematic phase LCs, can act as linear polarisers or even controllable quarter or half wave plates, based on their orientation or rotation as a function of plane crystal surface, as used for 3D projection. Here, the situation is different; chiral circularly polarised emitters are used with a linear polariser: the incident angle of circularly polarised light is always 1/8th of the wavelength with respect to the axis of travel to the polariser at a point (rather than a slit, with linear polarised light). Rotating a linear polariser in the detection set-up, with circularly polarised emitted light does not make any contrast difference as a function of rotation angle.

In this example, broad spectrum circularly polarised light is translated to well-defined linearly polarised light (using the birefringent quarter-wave plate and the linear polariser). In this set up two linear polarisers, aligned at a predetermined relative angle, separate the horizontal and vertical linearly polarised light generated; the H-LPL and V-LPL are a direct, wavelength-independent representation of the initially emitted left and right handed CP light. This study therefore suggests a role for applications using the strong CPL emission of such Eu complexes in security tagging, among other possibilities.

We would like to acknowledge the ERC (FCC 266804), EPSRC and the Royal Society (RP) for support, and Prof. Andrew Beeby for fruitful discussions and invaluable help concerning the optical set up.

Notes and references

- 1 F. Zinna and L. Di Bari, *Chirality*, 2015, **27**, 1.
- 2 J. P. Riehl and F. S. Richardson, *Chem. Rev.* 1986, **86**, 1.
- 3 R. Carr, N. H. Evans and D. Parker, *Chem. Soc. Rev.* 2012, **41**, 7673.
- 4 S. D. Pietro and L. Di Bari, *Inorg. Chem.* 2012, **51**, 12007.
- 5 a) J.-C. G. Bunzli, *Chem. Rev.* 2010, **110**, 2729; b) M. C. Heffern, L. M. Matosiuk and T. J. Meade, *Chem. Rev.* 2014, **114**, 4496; c)
- 6 a) E. G. Moore, A. P. S. Samuel and K. N. Raymond, *Acc. Chem. Res.* 2009, **42**, 542; b) J. Xu, T. M. Corneille, E. G. Moore, G.-L. Law, N. G. Butlin and K. N. Raymond, *J. Am. Chem. Soc.*, 2011, **133**, 19900.
- 7 S. J. Butler, L. Lamarque, R. Pal and D. Parker, *Chem. Sci.*, 2014, **5**, 1750.
- 8 A.-S. Chauvin, S. Comby, B. Song, C. D. B. Vandevyver, F. Thomas and J.-C. G. Bunzli, *Chem. – Eur. J.*, 2007, **13**, 9515.
- 9 a) J. W. Walton, L. Di Bari, D. Parker, G. Pescitelli, H. Puschmann, D. S. Yufit, *Chem. Commun.* 2011, **47**, 12289; b) J. W. Walton, R. Carr, N. H. Evans, A. M. Funk, A. M. Kenwright, D. Parker, D. S. Yufit, M. Botta, S. De Pinto and K. L. Wong, *Inorg. Chem.*, 2012, **51**, 8042.
- 10 M. Delbianco, V. Sadovnikova, E. Bourrier, G. Mathis, L. Lamarque, J. M. Zwieter, D. Parker, *Angew. Chem. Int. Ed. Engl.* 2014, **53**, 10718.
- 11 M. Soulie, F. Latzko, E. Bourrier, V. Placide, S. J. Butler, R. Pal, J. W. Walton, P. L. Baldeck, B. Le Guennic, C. Andraud, J. M. Zwieter, L. Lamarque, D. Parker and O Maury, *Chem. Eur. J.* 2014, **20**, 8636.
- 12 S. J. Butler, M. Delbianco, L. Lamarque, B. K. McMahon, E. R. Neil, R. Pal, D. Parker, J. W. Walton, J. M. Zwieter, *Dalton Trans.* 2015, **44**, 4791.
- 13 E. R. Neil, M. A. Fox, R. Pal and D. Parker, *Dalton Trans.* 2016, **45**, 8355.
- 14 a) N. H. Evans, R. Carr, M. Delbianco, R. Pal, D. S. Yufit, D. Parker, *Dalton Trans.* 2013, **42**, 15610; b) E. R. Neil, A. M. Funk, D. S. Yufit and D. Parker, *Dalton Trans.*, 2014, **43**, 5490; c) S. J. Butler, M. Delbianco, N. H. Evans, A. T. Frawley, R. Pal, D. Parker, R. S. Puckrin and D. S. Yufit, *Dalton Trans.*, 2014, **43**, 5721.
- 15 R. Pal and A. Beeby, *Methods Appl. Fluoresc.*, 2014, **2**, 037001.

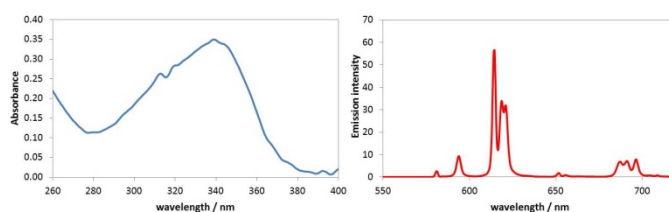
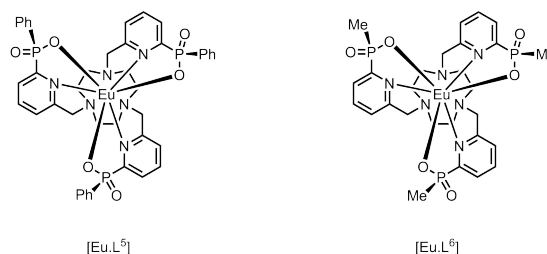


Figure 1 Absorption and emission spectra for [Eu.L⁴] (MeOH, 295 K), showing the fingerprint Eu emission profile arising from transitions from ⁵D₀ to the ⁷F_n manifold (n = 0-4 shown here)

Table 1 Key photophysical properties of the europium(III) complexes (295 K, MeOH)

Complex	λ_{\max}^a / nm	Normalised absorbance at 365 nm / %	Φ_{em} / %	τ_{Eu} / ms
[Eu.L ¹]	356	98	50	1.18
[Eu.L ²]	343	40	47	1.22
[Eu.L ³]	355	100	55	1.10
[Eu.L ⁴]	342	37	54	1.14

^a Extinction coefficients for these complexes are 65,000 ($\pm 5,000$) M⁻¹ cm⁻¹



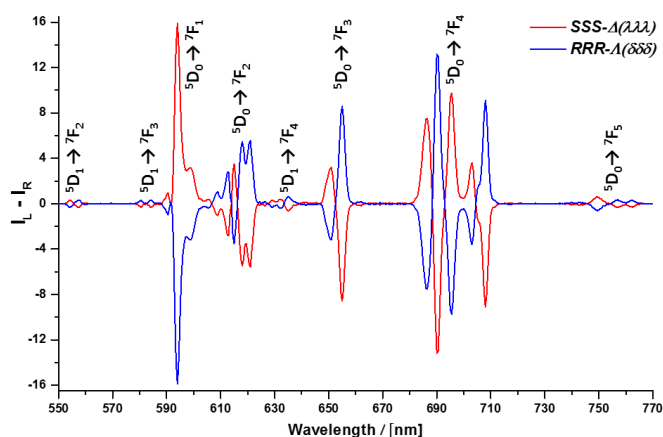
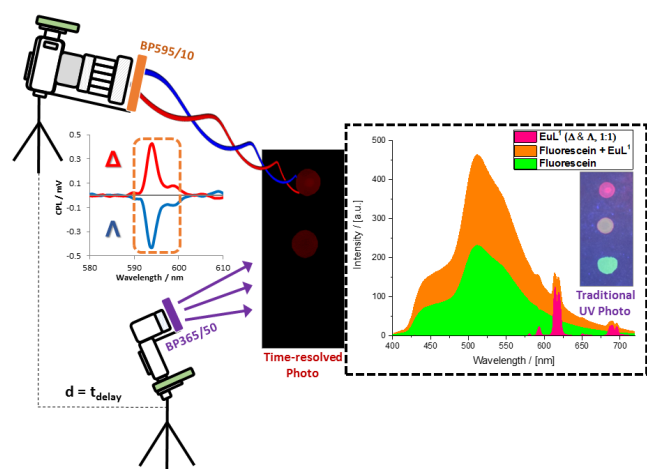


Figure 2 Circularly polarised luminescence spectra for the enantiomers of $[\text{Eu.L}^2]$ (red Δ ; blue Λ) ($5 \mu\text{M}$ complex, 4 min acquisition time, 3 averages, MeOH, 295 K; see ESI for g_{em} values).



Scheme 1 Schematic set-up and proof-of-concept for time-resolved image separation using off-the shelf DSLR equipment. The three spots in the paper sample are: Λ & Δ - $[\text{Eu.L}^2]$ (1:1) (*top*); Λ & Δ - $[\text{Eu.L}^2]$ (1:1) and fluorescein (*centre*) and fluorescein only (*bottom*). The time resolved image cuts out the fluorescein emission; the applied band-pass filter selects the spectral part of interest, as further separated with respect to sign by the parallel chiroptical image analysis (*in microscopy*, Figure 3).

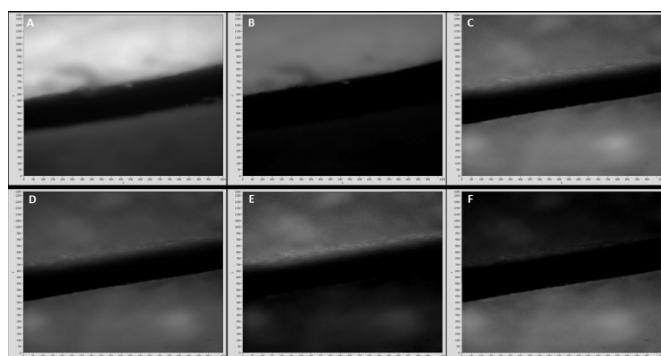


Figure 3. Microscopy images following sample excitation using a 365 nm UV-LED ($t_{\text{acq.}} = 7.2 \text{ ms/frame}$, 395 nm dichroic mirror, λ_{em} LP-420 nm) of fluorescein, Λ - and Δ - europium(III) complex recorded on a custom-built microscope incorporating a chiroptical selector unit. (A) Ungated image of (*top*) Λ - and Δ - $[\text{Eu.L}^2]$ (1:1) and (*bottom*) fluorescein, using 10 frame accumulation imaging sequence. (B) Time-

resolved image of (*top*) Λ - and Δ - $[\text{Eu.L}^2]$ (1:1) and (*bottom*) fluorescein ($t_d = 6 \mu\text{s}$, λ_{em} LP-420 nm, 50 frame acc.). (C) Time-resolved image of (*top*) Λ - $[\text{Eu.L}^2]$ and (*bottom*) Δ - $[\text{Eu.L}^2]$ using ($t_d = 6 \mu\text{s}$, λ_{em} LP 420 nm, 70 acc.). (D) Time-resolved image of (*top*) Δ - $[\text{Eu.L}^2]$ and (*bottom*) Λ - $[\text{Eu.L}^2]$ ($t_d = 6 \mu\text{s}$, λ_{em} BP 595/10 nm, 150 frame acc.). (E) Time-resolved image of (*top*) Λ - $[\text{Eu.L}^2]$ and (*bottom*) Δ - $[\text{Eu.L}^2]$ using the RIGHT (horizontal polarisation) circularly polarised light chiroptical channel ($t_d = 6 \mu\text{s}$, λ_{em} BP-589/20 nm, 370 frame acc.). (F) Time-resolved image of (*top*) Λ - $[\text{Eu.L}^2]$ and (*bottom*) Δ - $[\text{Eu.L}^2]$, using the dedicated LEFT (vertical polarisation) circularly polarised light channel ($t_d = 6 \mu\text{s}$, λ_{em} BP-589/20 nm, 370 frame acc.).